Catena 137 (2016) 161–172

Contents lists available at ScienceDirect

Catena

journal homepage: www.elsevier.com/locate/catena

Spatio-temporal analysis of rainfall erosivity and erosivity density in Greece

Panos Panagos [a,*], Cristiano Ballabio [a], Pasquale Borrelli [a], Katrin Meusburger [b]

[a] European Commission, Joint Research Centre, Institute for Environment and Sustainability, Via E. Fermi 2749, I-21027 Ispra VA, Italy
[b] Environmental Geosciences, University of Basel, Switzerland

ARTICLE INFO

Article history:
Received 25 September 2014
Received in revised form 16 September 2015
Accepted 23 September 2015
Available online 3 October 2015

Keywords:
R-factor
Seasonality
Rainfall intensity
Monthly erosivity density
Soil erosion
RUSLE

ABSTRACT

Rainfall erosivity considers the effects of rainfall amount and intensity on soil detachment. Rainfall erosivity is most commonly expressed as the R-factor in the Universal Soil Loss Equation (USLE) and its revised version, RUSLE. Several studies focus on spatial analysis of rainfall erosivity ignoring the intra-annual variability of this factor. This study assesses rainfall erosivity in Greece on a monthly basis in the form of the RUSLE R-factor, based on a 30-min data from 80 precipitation stations covering an average period of almost 30 years. The spatial interpolation was done through a Generalised Additive Model (GAM). The observed intra-annual variability of rainfall erosivity proved to be high. The warm season is 3 times less erosive than the cold one. November, December and October are the most erosive months contrary to July, August and May which are the least erosive. The proportion between rainfall erosivity and precipitation, expressed as erosivity density, varies throughout the year. Erosivity density is low in the first 5 months (January–May) and is relatively high in the remaining 7 months (June–December) of the year. The R-factor maps reveal also a high spatial variability with elevated values in the western Greece and Peloponnesus and very low values in Western Macedonia, Thessaly, Attica and Cyclades. The East–West gradient of rainfall erosivity differs per month with a smoother distribution in summer and a more pronounced gradient during the winter months. The aggregated data for the 12 months result in an average R-factor of 807 MJ mm ha^{-1} h^{-1} $year^{-1}$ with a range from 84 to 2825 MJ mm ha^{-1} h^{-1} $year^{-1}$. The combination of monthly R-factor maps with vegetation coverage and tillage maps contributes to better monitor soil erosion risk at national level and monthly basis.

1. Introduction

Soil erosion is serious environmental and public health problem that human society is facing, as every year at global scale almost 10 ha of cropland are lost due to soil erosion (Pimentel, 2006). To design efficient policies, land use planners and decision makers need, among others, information on the on-site private costs and the offsite consequences (desertification, rural depopulation, siltation of waterways and reductions in biodiversity) plus data on soil erosion (Colombo et al., 2005).

The empirical Revised Universal Soil Loss Equation (RUSLE) (Renard et al., 1997), which predicts the average annual soil loss resulting from raindrop splash and runoff from field slopes, has widely been used as a tool for predicting soil erosion at large spatial scales (Kinnell, 2010; Panagos et al., 2015a). Among the factors used within RUSLE, the rainfall is accounted by rainfall erosivity (R-factor) which combines the influence of precipitation duration, magnitude and intensity. The R-factor is a multi-annual average index that measures rainfall's kinetic energy and intensity to describe the effect of rainfall on sheet and rill erosion (Wischmeier and Smith, 1978).

Of all the erosion factors, rainfall erosivity and land cover/management factor are considered to be the most dynamic. By capturing the variability of those two factors, it is possible to have a more realistic and precise soil erosion assessment. For instance, a rainstorm may cause severe soil loss in the fallow period but hardly any damage during the growing season. A monthly estimation of precipitation and rainfall intensity has been used for assessing the temporal variability of rainfall erosivity in Ethiopia (Nyssen et al., 2005) and Switzerland (Meusburger et al., 2012). Furthermore, the spatial and the temporal variability of the R-factor have been important in risk assessments in Andalusia (Renschler et al., 1999) and in recent developments of G2 soil erosion model in Strymonas catchment (Panagos et al., 2012) and Crete (Panagos et al., 2014).

As for rainfall erosivity, Greece is a very interesting study area due to the high climate diversity mainly attributed to high relief variability. The main objective of this study is to assess the spatio-temporal variability

* Corresponding author.
E-mail address: panos.panagos@jrc.ec.europa.eu (P. Panagos).

http://dx.doi.org/10.1016/j.catena.2015.09.015

of rainfall erosivity in Greece based on precipitation data with a high temporal resolution. Specific aims of this study are to:

a) compute monthly rainfall erosivity on 80 precipitation stations in Greece;
b) produce linear regression functions that can predict monthly R-factor on station basis;
c) interpolate station R-factor values to produce 12 monthly R-factor maps using a Generalised Adaptive Model and spatial covariates which among others can potentially be used for monthly soil erosion modelling; and
d) identify spatial and temporal patterns to map the relationship between the R-factor and the precipitation (monthly erosivity density).

2. Data and methods

2.1. Study area

Greece is classified as Mediterranean climate type according to Köpper classification (Kööppen, 1918): mild and rainy winters, relatively warm and dry summers, and l extended periods of sunshine throughout most of the year. The orographic and topographic influences, along with the influence of the Mediterranean waters (warmer than the adjoining land in winter and cooler in summer) cause an uneven temporal and spatial distribution of precipitation (Hatzianastassiou et al., 2008).

WorldClim statistics (Hijmans et al., 2005) reports 698 mm as the mean annual precipitation, 189 mm as the standard deviation, and from 380 to 1406 mm as the range of annual precipitation values in the study area (Fig. 1). The weather in Greece varies from the dry climate of Attica (Athens' greater area) and of East Greece, to the wet climate of Northern and Western Greece (HNMS, 2014).

In Greece, the year can be broadly subdivided into two main seasons: The cold and rainy period lasting from mid-October until the end of March, and the warm and dry season lasting from April until September. The wettest months are January (94.8 mm) and December (107.6 mm), whereas the driest ones are July (19.6 mm) and August (16.3 mm) according to the WorldClim data. The precipitation regime in Greece has been extensively studied in past, further climatic details are provided by Bartzokas et al., 2003; Tolika and Maheras, 2005; Pnevmatikos and Katsoulis, 2006.

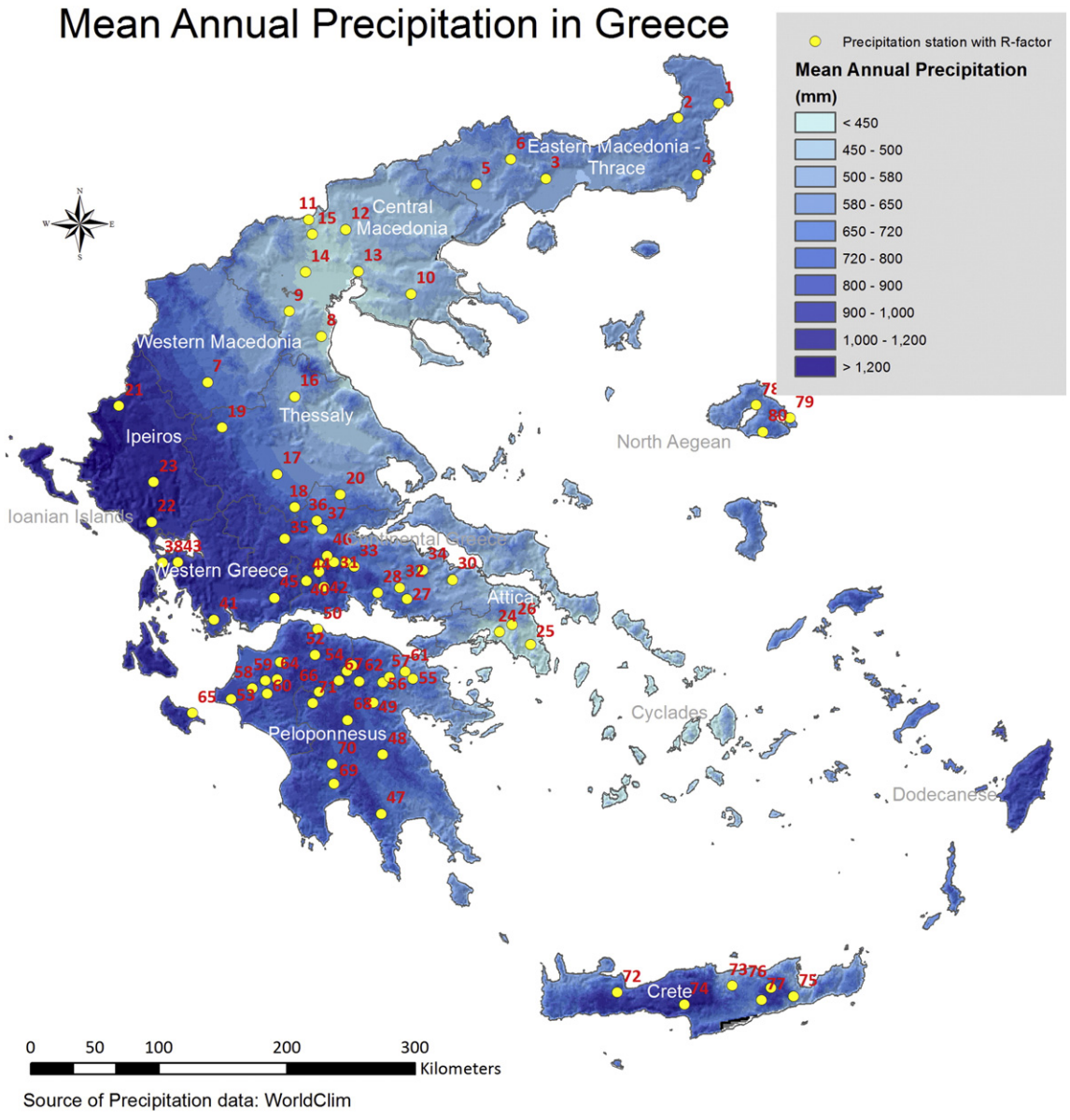

Fig. 1. Spatial distribution of mean annual precipitation and stations (Numbers refer to the station id in the Appendix) used for the R-factor calculation in Greece.

2.2. Precipitation data collection

High-resolution precipitation datasets (30 min) have been extracted from 80 stations: 77 precipitation stations from the database of the research project Hydroscope, and 3 stations from the database of the Aegean University. Hydroscope is a Greek nation-wide research programme aiming at developing a database system for meteorological, hydrological and hydrogeological information at national level (Sakellariou et al., 1994). Regarding the spatial distribution of the precipitation stations with high resolution data, the average density is ca. 1 station per 40 km × 40 km grid cell (Fig. 1).

There is a quite dense network of precipitation stations in Peloponnesus and in the Continental Greece, whereas there is a lack of stations in Western Macedonia and in the Aegean Islands. According to the Nomenclature of Territorial Units for Statistics (NUTS), precipitation stations are located in 33 out of the 51 Greek prefectures (NUTS3 level) (Appendix). The stations are located at different altitudes so as to represent the huge topographic variability in Greece.

Regarding the temporal resolution, the data have been collected from 2373 years for 29.7 years per station on average. The mean annual and monthly rainfall erosivity of each station is calculated based on long-term time series, preferably more than 15 years (Foster et al., 2008). So, 64 precipitation stations (80% of the total) recorded data covering at least 20 years and starting from middle 1970s up to the year 1996 (Appendix). Among the rest 20% (shorter time-series), it was preferred to include the 3 precipitation stations from Lesvos island and 4 ones from Crete island in order to reduce the spatial uncertainty due to complete lack of data in the Aegean Islands.

2.3. R-factor calculation

The original RUSLE R-factor Eq. (1) was used to create the R-factor database of 12 monthly values per 80 precipitation stations (960 records) in Greece. The R-factor is the product of kinetic energy of a rainfall event (E) and its maximum 30-min intensity (I_{30}) (Brown and Foster, 1987):

$$R = \frac{1}{n}\sum_{j=1}^{n}\sum_{k=1}^{mj}(EI_{30})_k \quad (1)$$

where: R is the average monthly rainfall erosivity (MJ mm ha^{-1} h^{-1} $month^{-1}$); n is the number of years recorded; m_j is the number of erosive events during a given month j; and EI_{30} is the rainfall erosivity index of a single event k. The event erosivity EI_{30} (MJ mm ha^{-1} h^{-1}) is defined as:

$$EI_{30} = \left(\sum_{r=1}^{m} e_r v_r\right) I_{30} \quad (2)$$

Where e_r is the unit rainfall energy (MJ ha^{-1} mm^{-1}) and v_r the rainfall volume (mm) during r-th period of a storm which divided into m parts. I_{30} is the maximum rainfall intensity during a 30-min period of the rainfall event (mm h^{-1}). The 30 min temporal resolution of precipitation data leads to around 20% underestimation of maximum rainfall intensity compared to very high resolution (5 min) and as a consequence to lower R-factor values (Panagos et al., 2015b).

The unit rainfall energy (e_r) is calculated for each time interval as follows (Brown and Foster, 1987):

$$e_r = 0.29[1-0.72\exp(-0.05i_r)] \quad (3)$$

where i_r is the rainfall intensity during the time interval (mm h^{-1}).

The sums of EI_{30} and the average R-factor have been calculated on a monthly basis. The erosive events have been selected based on the three criteria of Renard et al. (1997) followed by Panagos et al. (2015b).

2.4. Spatial interpolation of the R-factor

In the late 1990's Goovaerts (1999) introduced a geo-statistical interpolation method to calculate rainfall erosivity based on regionalised variables such as elevation. Rainfall erosivity is mainly correlated with climatic data and, especially, with the amount of precipitation, the elevation and the geographical position (x, y coordinates).

A series of twelve Generalised Additive Models (GAM) have been used to predict the corresponding monthly R-factor datasets. GAMs are a generalization of linear regression models in which the coefficients can be expanded as link functions, typically splines, of covariates (Hastie and Tibshirani, 1986). GAMs are semi-parametric and can account for some non-linear relationships between dependent variable and covariates. In this study, thin plate regression splines served as link functions and were fitted by maximum penalized likelihood (Wood, 2006). For each of the twelve months a GAM model was fitted using the average rainfall of that given month, elevation and spatial coordinates as candidate covariates. Each model was then further expanded by subsequently including other months' rainfall data. Subsequently a stepwise backward approach was used to select the best set of covariates and to determine the relative influence of each of the covariates on the overall model performance. Spatial covariates were treated as a bivariate covariate, thus resulting in a 2 dimensional spline representing the spatial variation unaccounted by other covariates. The choice of using a 2d spline instead of kriging is due to the better estimation of the spatial correlation with a limited set of points.

2.5. Covariates for spatial interpolation

Three main covariates were considered for the GAM regression model as being significant:

1. *average monthly precipitation* derived from the WorldClim database (Hijmans et al., 2005), which reports monthly averages of precipitation and temperature for the period 1950–2000 at 1000 m × 1000 m resolution;
2. *elevation* derived from the Digital Elevation Model of the Shuttle Radar Topography Mission (SRTM) at 100 m × 100 m resolution; and
3. *latitude and longitude*.

2.6. Erosivity density calculation

The erosivity density is the ratio of R-factor to precipitation (Kinnell, 2010) and in practice measures the erosivity per rainfall unit (mm), and is expressed as MJ ha^{-1} h^{-1}. Monthly precipitation (P) data have been extracted from the WorldClim database (Hijmans et al., 2005) and monthly rainfall erosivity (R) data are the outputs of the R-factor spatial interpolation. At a pixel level, the erosivity density (ED) for a given month j is:

$$ED_j = R_j/P_j \quad (4)$$

3. Results and discussion

This section will address three issues: a) the seasonal rainfall erosivity per station and how this can produce extrapolating regression functions to stations with low resolution (e.g. monthly) data b) the mapping of monthly rainfall erosivity using spatial interpolation and its further application in estimating soil erosion risk and c) the seasonal erosivity density assessment.

3.1. Seasonal rainfall erosivity per station

The mean R-factor of the 80 precipitation stations is 849.6 MJ mm ha^{-1} h^{-1} $year^{-1}$ (Table 1) with a high standard deviation

Table 1
Seasonal and annual R-factor per precipitation station.

Map Id	Station name	Winter (Dec–Jan–Feb)	Spring (Mar–Apr–May)	Summer (Jun–Jul–Aug)	Autumn (Sep–Oct–Nov)	Annual R-factor
		(MJ mm ha^{-1} h^{-1} $year^{-1}$)				
1	Didimoticho	111.2	138.9	112.7	197.3	560.0
2	Mikro Dereio	116.4	97.3	204.4	334.1	752.2
3	Toxotes	321.4	102.3	102.1	235.9	761.7
4	Ferres	282.3	177.4	190.6	429.8	1080.1
5	Drama	69.7	89.3	107.6	111.0	377.6
6	Paranesti	140.9	101.6	151.7	173.4	567.6
7	Grevena	64.5	60.4	57.5	94.5	276.8
8	Katerini	68.0	100.4	80.8	239.6	488.8
9	Fragma Aliakmona	67.1	125.2	40.2	142.1	374.5
10	Agios Prodromos	40.8	72.1	92.8	96.8	302.5
11	Euzonoi	41.6	77.4	87.0	84.8	290.8
12	Kilkis	54.4	80.4	183.5	105.7	424.0
13	Oraiokastro	46.4	80.1	236.4	114.3	477.3
14	Paralimni Giannitsa	35.5	66.4	76.5	156.1	334.5
15	Polikastro	75.2	91.8	174.7	137.7	479.4
16	Elassona	35.2	109.4	114.6	151.2	410.4
17	Karditsa	68.3	76.4	99.3	114.5	358.4
18	Loutropigi	132.5	123.5	123.7	296.8	676.5
19	Megali Kerasia	102.3	69.7	59.6	131.3	362.9
20	Skopia	64.2	66.1	83.2	140.8	354.3
21	Basiliko	193.2	113.1	75.0	380.9	762.2
22	Louros	890.0	292.3	48.8	723.2	1954.3
23	Pentolakos	1319.3	537.6	403.2	1349.2	3609.2
24	Nikaia-Egaleo	160.5	71.0	20.3	85.5	337.2
25	Markopoulo	167.1	69.7	12.5	103.1	352.3
26	Chalandri	149.6	45.2	10.8	124.8	330.5
27	Agia Triada	310.1	187.1	51.7	270.6	819.5
28	Distomo	179.2	79.9	51.3	200.4	510.8
29	Gravia	278.7	119.1	98.0	367.8	863.5
30	Limni Ilikis	93.0	41.1	14.0	123.8	271.9
31	Kaloskopi	504.8	120.4	198.3	531.8	1355.2
32	Livadia	229.1	115.0	120.2	314.8	779.1
33	Lilaia	309.9	162.4	197.3	397.4	1067.1
34	Pavlos	129.2	65.6	42.9	147.8	385.5
35	Timfristos	520.6	297.0	84.6	464.2	1366.4
36	Trilofo	89.0	54.6	40.7	121.5	305.7
37	Zilefto	75.9	56.9	71.3	171.7	375.7
38	Agios Nikolaos	304.1	173.9	76.3	871.4	1425.7
39	Athan. Diakos	748.0	295.0	185.8	639.8	1868.7
40	Koniakos	665.7	150.4	24.7	326.3	1167.1
41	Lesinio	209.5	68.3	22.4	430.5	730.5
42	Lidoriki	385.1	146.4	69.1	384.5	985.1
43	Monastiraki	226.1	127.4	37.9	421.2	812.6
44	Pentagioi	983.0	357.2	149.3	554.3	2043.8
45	Poros Rigani	856.3	326.1	90.6	707.1	1980.0
46	Pyra	336.7	155.9	200.0	361.7	1054.3
47	Arna	986.5	260.2	63.7	691.8	2002.3
48	Karyes	170.7	98.5	39.4	129.5	438.1
49	Neochori	284.5	124.5	201.1	451.9	1062.0
50	Aigio	253.8	102.2	23.0	332.6	711.7
51	Asteri	119.4	105.8	75.9	254.9	555.9
52	Drossato	254.2	124.5	115.8	344.6	839.0
53	Gastouni	474.8	174.2	45.1	750.3	1444.3
54	Kalivia -Feneos	524.4	145.0	194.6	432.4	1296.4
55	Klenia	266.0	147.4	151.8	315.5	880.7
56	Leontio	201.5	153.4	104.9	83.5	543.3
57	Nemea	372.3	155.5	75.2	236.1	839.1
58	Fragma Pinios	233.5	70.9	44.5	277.4	626.4
59	Portes	478.5	228.6	76.9	880.5	1664.4
60	Simopoulo	200.9	99.1	64.5	261.3	625.8
61	Spathovouni	192.8	68.8	100.5	131.4	493.4
62	Lafka Stimfalaia	152.2	83.0	56.2	147.3	438.7
63	Tarsos	257.8	152.3	128.5	305.3	844.0
64	Ksirochorio	222.6	290.0	119.3	504.0	1135.9
65	Zakinthos	425.0	144.9	38.9	677.7	1286.5
66	Dafni	398.0	109.8	27.2	203.3	738.2
67	Lykouria	90.1	64.7	36.9	112.3	304.0
68	Piana	606.9	229.0	214.8	578.9	1629.5
69	Pidima	577.1	166.1	62.5	663.0	1468.6
70	Souli	562.8	177.4	76.7	719.4	1536.4
71	Tropaia	169.2	85.6	77.5	235.0	567.4
72	Ebrosneros	555.7	360.5	14.4	312.1	1242.6
73	Ano Archanes	341.2	113.6	8.2	205.3	668.3

Table 1 (*continued*)

Map Id	Station name	Winter (Dec–Jan–Feb)	Spring (Mar–Apr–May)	Summer (Jun–Jul–Aug)	Autumn (Sep–Oct–Nov)	Annual R-factor
		(MJ mm ha^{-1} h^{-1} year^{-1})				
74	Nithafri	539.1	63.1	5.9	349.0	957.1
75	Kalamafka	318.1	34.3	0.0	111.2	463.6
76	Agios Georgios	217.4	84.8	0.0	305.3	607.4
77	Ebaros-Anapodiaris	330.7	54.8	0.0	147.4	533.0
78	Agia Paraskevi	165.7	69.8	232.5	66.1	534.0
79	Panepistimio Aegean	498.4	137.4	16.3	208.7	860.7
80	Akrasi	564.5	185.8	7.0	146.2	903.5
Average		303.2	135.1	90.9	320.4	849.6

of 564.2 MJ mm ha^{-1} h^{-1} year^{-1} as expected due to the high climate variability and high topographic diversity. The smallest R-factors (<300 MJ mm ha^{-1} h^{-1} year^{-1}) were calculated in two stations in Central and Western Macedonia (Grevena, Evzonoi) and in Viotia (Lake Iliki). The maximum values was calculated in Western Ipeiros (Pentolakos) with a value higher than 3500 MJ mm ha^{-1} h^{-1} year^{-1} followed by 2 stations having values over 2000 MJ mm ha^{-1} h^{-1} year^{-1} (Pentagioi Fokidas in Continental Greece, Arna in western Peloponnesus).

According to the individual stations' monthly R-factor, autumn is the most erosive period with an average of 320.4 MJ mm ha^{-1} h^{-1} year^{-1}, followed by winter with 303.2 MJ mm ha^{-1} h^{-1} year^{-1}, spring with an average of 135.1 MJ mm ha^{-1} h^{-1} year^{-1} and summer with 90.9 MJ mm ha^{-1} h^{-1} year^{-1}. In practice 73% of the rainfall erosivity takes place in autumn and winter.

R-factor values can potentially be extrapolated to additional precipitation stations with low temporal resolution data (Bonilla and Vidal, 2011). The relatively high number of stations with monthly R-factor data allow to develop regression functions per month (Table 2). Those equations are potentially applicable in Greece to predict monthly R-factor values for stations with available long time-series of monthly precipitation data. We tried to include monthly precipitation ($Prec_{Month}$), latitude(y), longitude(x) and elevation (Elev) as input attributes for getting the monthly regression functions at a p value <0.05.

Average monthly precipitation is always significant in the monthly regression functions while the longitude(X) has not been significant (Table 2). The effect of elevation is inter-correlated to precipitation. For the summer period the latitude is significant as southern areas have higher R-factor values. The uncertainty is relatively higher for the equations predicting R-factor during May and August while the wet months (October, November, December, January and February) have less uncertainty. The coefficients of precipitation in those regression functions show that R-factor during the period May to December is more 'sensitive' to precipitation compared to the period January–April. However, those extrapolation functions are not recommended for spatial interpolation. Moreover, we recommend potential users to apply those equations with caution as they are empirical and location dependant (Oliveira et al., 2013).

Table 2
Regression functions for monthly R-factor estimation of individual stations (Prec: Precipitation; Elev: Elevation; Y: Latitude).

Period	Regression functions from individual stations	R^2
January	$-39.1 + 1.8*Prec_{January}$	0.84
February	$-37.5 + 1.65*Prec_{February}$	0.81
March	$-34.4 + 1.65*Prec_{March}$	0.64
April	$-22.5 + 1.5*Prec_{April}$	0.76
May	$259 + 2.2*Prec_{May} - 0.026*Elev - 7.3*Y$	0.58
June	$-6.6 + 2.1*Prec_{June}$	0.71
July	$243 + 3.2*Prec_{July} - 6.7*Y$	0.71
August	$242 + 3.1*Prec_{August} - 6.5*Y$	0.51
September	$228 + 3.5*Prec_{September} - 0.015*Elev - 6.65*Y$	0.7
October	$275 + 3.3*Prec_{October} - 0.08*Elev - 8.2*Y$	0.84
November	$-78.9 + 2.96*Prec_{November} - 0.04*Elev$	0.81
December	$-79 + 2.45*Prec_{December}$	0.78

3.2. Monthly maps of rainfall erosivity in Greece

The 12 maps of monthly rainfall erosivity in Greece (Fig. 2) show a gradient of high erosivity in Western Greece, Ionian Islands, Peloponnesus and western Crete to lower erosivity in Northern Greece, Thessaly, Attica and the Cyclades islands. The spatial resolution of the maps is at 100 m as all selected covariates (WorldClim, DEM) were available at this resolution. Using the covariates at high resolution, we avoided to resample them at coarser resolution and as a consequence to generate artefacts (Ballabio et al., 2014). The Generalised Adaptive Model (GAM) used for the interpolation of the monthly erosivity point data showed a good performance in most of the months with the exception of May, July, August and September (Table 3). This confirms the difficulty to predict rainfall erosivity based on few rainstorms in summer.

Since the spatial interpolation was performed with GAM, the spline functions may be presented only in a graphical way. In addition, a linear regression was applied, however, the Linear Model (LM) performed worse than GAM according to the coefficient of determination R^2 (Table 3). Precipitation is the slope (β_1) and β_0 is the intercept of the Linear Model (LM).

The highest mean R-factor is noticed in November (144.6 MJ mm ha^{-1} h^{-1} month^{-1}), December (136.2 MJ mm ha^{-1} h^{-1} month^{-1}) and October (111.8 MJ mm ha^{-1} h^{-1} month^{-1}) while the lowest values are found in August (32.3 MJ mm ha^{-1} h^{-1} month^{-1}), July (33.3 MJ mm ha^{-1} h^{-1} month^{-1}), May (36.3 MJ mm ha^{-1} h^{-1} month^{-1}) and June (37.1 MJ mm ha^{-1} h^{-1} month^{-1}). The rainfall erosivity is almost 3 times higher during the cold and wet season (October – March) compared to the warm and dry season (April–September). However, there are regions such as Western Macedonia and Thessaly where mean summer rainfall erosivity is almost equal to mean winter rainfall erosivity. On the contrary, western part of Greece, Ionian Islands, Western Crete and Dodecanese show a pronounced seasonal variability with mean winter R-factor 4–5 times higher than the summer one.

The aggregated annual R-factor map of Greece has an average value of 807.4 MJ mm ha^{-1} h^{-1} year^{-1} and a standard deviation of 527.7 MJ mm ha^{-1} h^{-1} year^{-1}. The range of R-factor in Greece is 84.2–2825 MJ mm ha^{-1} h^{-1} year^{-1} with few high values over 2000 MJ mm ha^{-1} h^{-1} year^{-1} (in western Greece). The general pattern of the R-factor in Greece (Fig. 3) is also in accordance with spatial variability rainfall intensity in Greece (Kambezidis et al., 2010). The mean annual R-factor in Crete Island is 846 MJ mm ha^{-1} h^{-1} year^{-1} (Fig. 3) which is ca. 8% higher than the one calculated in the application of G2 erosion model in Crete (Panagos et al., 2014).

The cross validation and the Root Mean Square Error (RMSE) by leaving always one station out were generally acceptable for the months which contribute to 60% of total annual rainfall erosivity (October, November, December and January) (Table 3). However, it should be

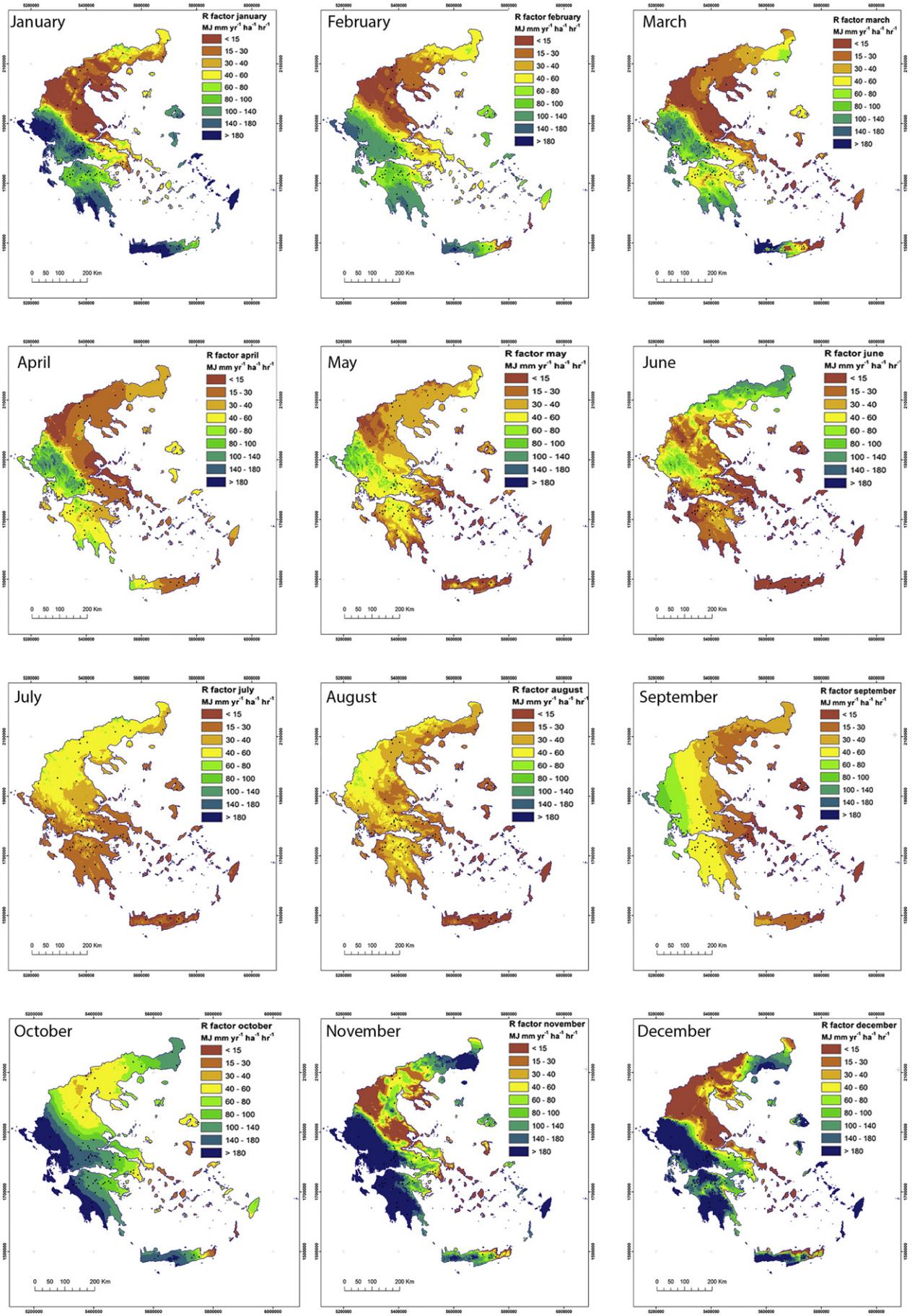

Fig. 2. High-resolution (100 m grid cell) monthly maps of rainfall erosivity (MJ mm ha^{-1} h^{-1} $month^{-1}$) in Greece.

Table 3
Performance of the spatial interpolation for each month (β_1 is the slope (precipitation) and β_0 is the intercept of the Linear Model).

Period	R^2 GAM	RMSE MJ mm ha^{-1} h^{-1} $month^{-1}$	R^2 cross validation	R^2 linear model (LM)	LM β_1	LM β_0
January	0.56	65.4	0.53	0.40	1.47	−59.16
February	0.43	52.64	0.25	0.30	1.21	−30.57
March	0.72	47.77	0.22	0.23	1.35	−39.85
April	0.51	29.99	0.22	0.27	1.34	−25.53
May	0.18	33.7	0.03	0.11	0.83	5.15
June	0.71	23.22	0.36	0.38	1.52	−7.58
July	0.12	32.26	0.24	0.11	1.23	9.83
August	0.14	30.14	0.03	0.05	1.05	17.34
September	0.28	32.85	0.21	0.22	1.78	−15.19
October	0.54	64.51	0.44	0.40	2.49	−65.58
November	0.65	66.47	0.55	0.47	3.22	−160.31
December	0.66	68.17	0.56	0.25	1.91	−84.60

noted that prediction at monthly temporal resolution has higher uncertainty than the prediction of annual R-factor. The standard error (Fig. 4) in combination with the mean R-factor values (Fig. 3) can be used for estimating the prediction intervals at a given confidence level. The prediction was found to have increased uncertainty levels in the Dodecanese Islands, Cyclades, Corfu and Western Macedonia due to lack of stations with rainfall erosivity data. An additional source of uncertainty is the different time spans from which R-factor is derived in the 80 precipitation stations. However, the long-time series (>20 years) of high temporal resolution precipitation data capture the R-factor trends and reduce this uncertainty.

3.3. Monthly erosivity density

Each monthly erosivity dataset (Fig. 2) is divided by the corresponding monthly precipitation dataset resulting in monthly erosivity density

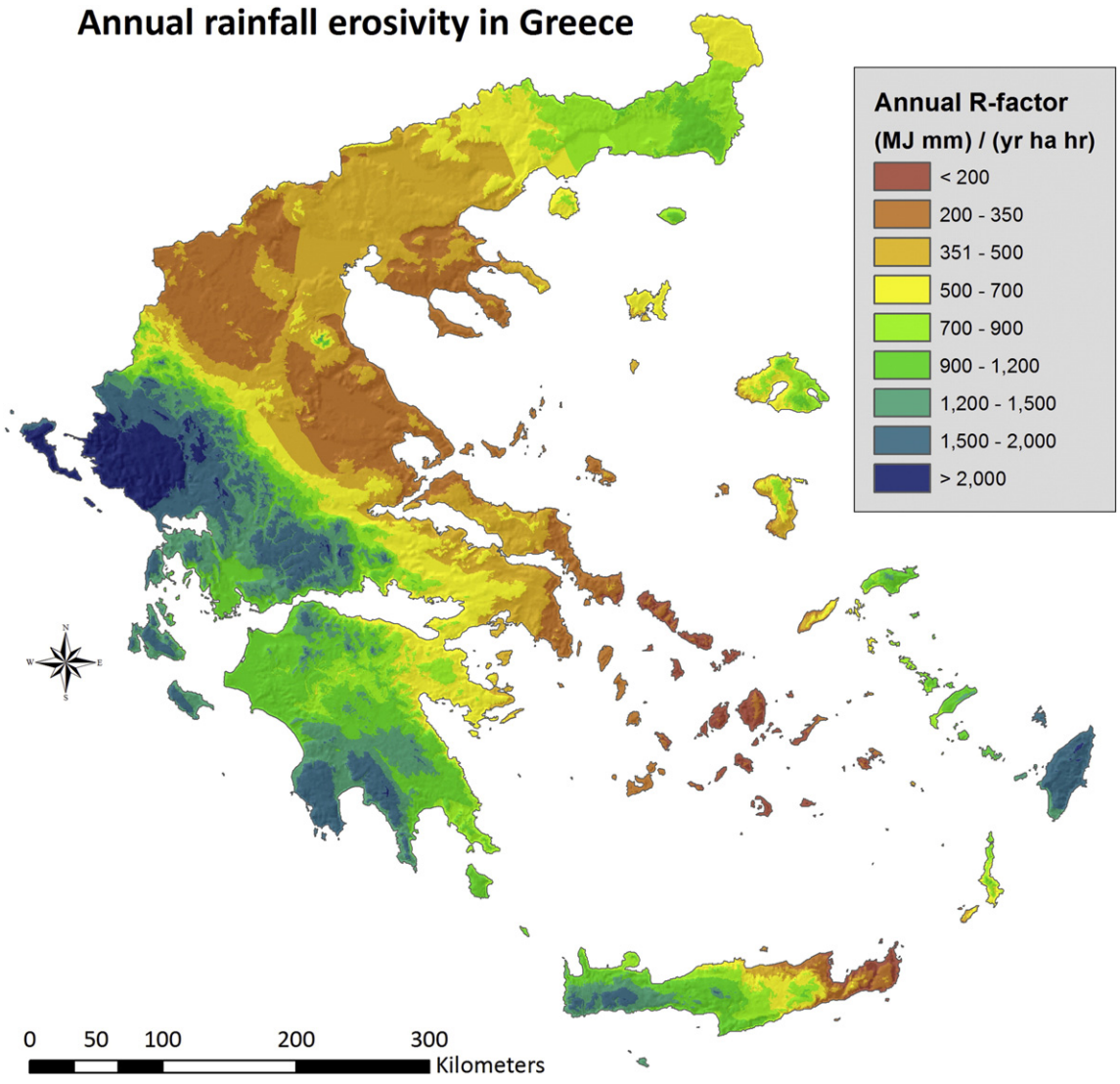

Fig. 3. High-resolution (100 m grid cell) annual map of rainfall erosivity (MJ mm ha^{-1} h^{-1} $year^{-1}$) in Greece.

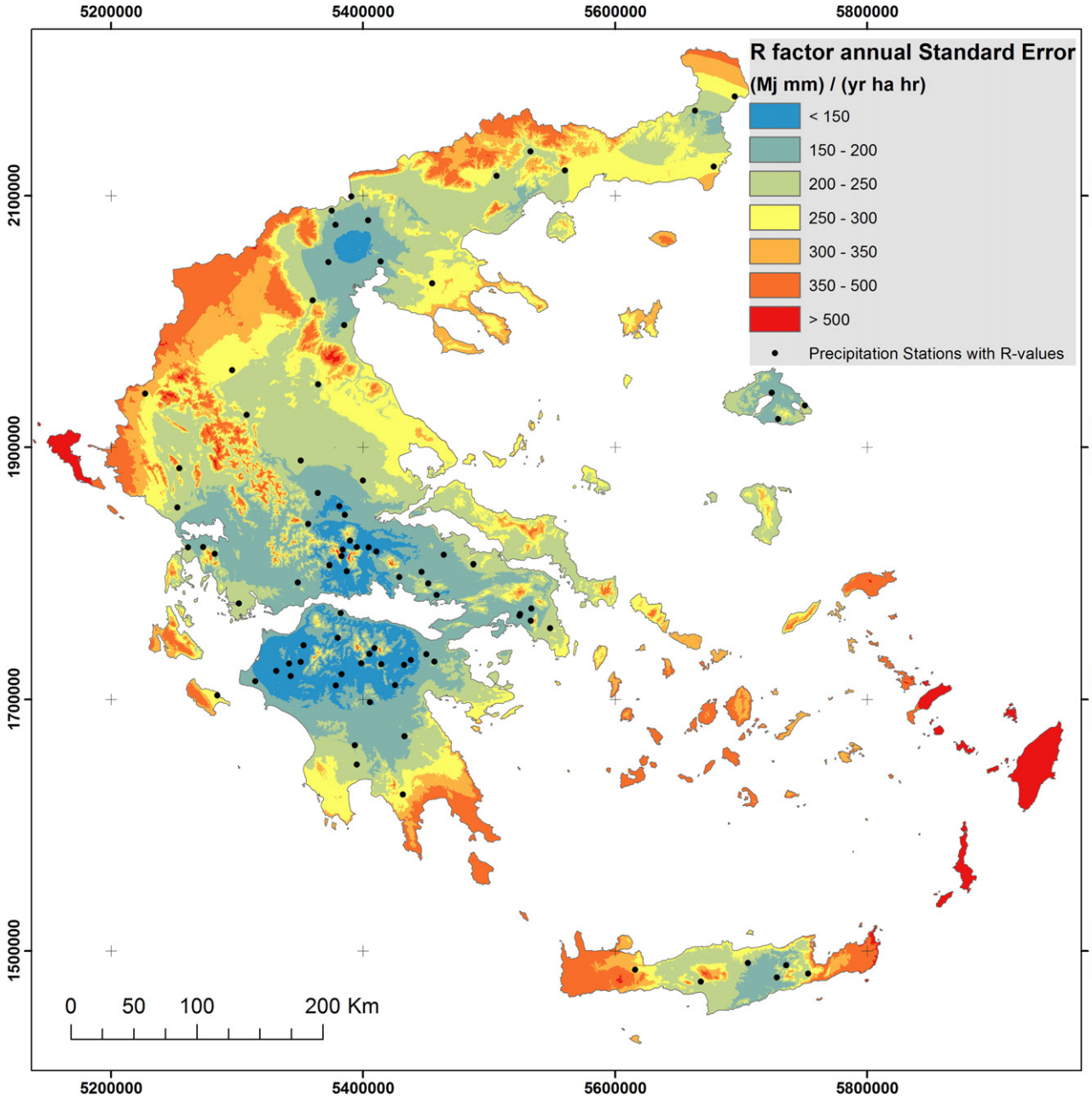

Fig. 4. Uncertainty of the R-factor prediction calculated with the GAM spatial interpolation model.

datasets. Erosivity density values higher than 1 mean that a certain precipitation amount may cause relatively higher rainfall erosivity. The erosivity density values are directly proportional to the average monthly 30-min rainfall intensity (Foster et al., 2008) and thus indicate the seasonal variation in rainfall intensity at a location. According to Dabney et al. (2011), very high monthly erosivity density values (>3 MJ ha^{-1} h^{-1}) significantly contribute to much higher predictions of runoff. This means that regions with high erosivity density are exposed to risk of flooding and even water scarcity as a result of their infrequent but very intense and erosive rainstorms.

For the first 5 months of the year (January to May), erosivity density (ED) is lower than 1 (Fig. 5) ranging from 0.76 to 0.87 due to the predominance of low intensity rainfall events. Starting from June the ED has an increasing trend during the summer months. Especially in August the average rainfall erosivity per precipitation amount is almost double compared to the annual average. High erosivity density months indicate that the precipitation is characterised by high intensity events of short duration (rainstorms). For example, January and November are the wettest months after December with similar mean rainfall amount (ca. 92–95 mm). However, mean R-factor in November is 50% higher compared to January which indicates that November has a higher number of rainstorms. In terms of erosivity, November is the most 'dangerous' month in Greece due to the highest R-factor combined with intense storms (elevated erosivity density).

The annual erosivity density has a mean value of 1.22 MJ ha^{-1} h^{-1}, with high variability ranging from 0.15 to 2.14 MJ ha^{-1} h^{-1}. The seasonal variability of erosivity density is also very high as the summer has the highest mean erosivity density with 1.89 MJ ha^{-1} h^{-1} followed by autumn with 1.36 MJ ha^{-1} h^{-1}, winter with 0.85 MJ ha^{-1} h^{-1} and spring with 0.78 MJ ha^{-1} h^{-1} (Fig. 6). The annual erosivity density spatial distribution is similar to the autumn erosivity density as this period is the most erosive one. The seasonal erosivity density reflects the rainfall intensity and indicates that there is relatively higher thunderstorm activity during summer and autumn (Fig. 6). In North Europe, intense

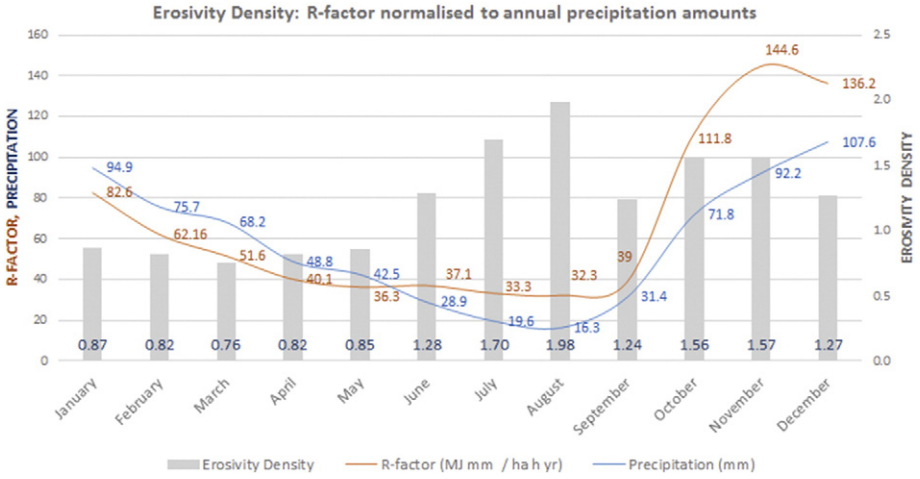

Fig. 5. Monthly R-factor, precipitation and erosivity density.

rainstorms fall between the end of spring and start of autumn (Diodato et al., 2014). In Greece, the intense rainstorms take place between July and December according to the erosivity density patterns (Fig. 6). The predominance of high erosivity density during summer and autumn is also confirmed with the spatial and temporal variation of lightning activity over Greece (Nastos et al., 2014).

Different spatial patterns of erosivity density are noticed during the four seasons. For example in Peloponnesus, the southern part has much higher values than northern for winter and spring while the west–east gradient is more visible in autumn and overall high values are noticed during summer. Moreover, the winter and spring have similar erosivity density in Greece but very different spatial patterns with lower variability in spring. The seasonal ED should be assessed together with the rainfall erosivity. North-East Greece and Crete have both high summer ED but Crete shows much lower erosivity in summer compared to the North-East Greece (Figs. 2 and 6). This high spatial and temporal variability of ED highlights the fact that rainfall erosivity is not solely dependent on the amount of precipitation. Consequently, it is impossible to predict spatially the monthly R-factor in Greece exclusively based on precipitation levels.

The erosivity density can also be used for estimating the R-factor for neighbouring (in a distance of few kilometres) stations having low resolution data (daily, monthly). However, this should be done carefully as assuming constant ED for a large region may produce mistakes due to high spatial and temporal variability of erosivity density.

The monthly, seasonal and annual erosivity density datasets (Fig. 6) are recommended (compared to the equations in Table 2) for the predictions of R-factor based on future climate change scenarios on the assumption that ED remains stable. To investigate the ED trend, we have calculated the average ED per 3 decades (1965–1974, 1975–1984 and 1985–1994) and its 9-year moving average for 8 representative stations (in terms of ED and R-factor) covering all geographic areas in Greece. During the period 1975–1984, it has been noticed an increase in ED followed by a lower decrease in the period 1985–1994 (see additional material). However, the limited time series (only 30-year data) and the lack of last 2 decades (1995–2014) do not allow to conclude a clear trend for erosivity density in Greece compared to the trend found in Ukkel (Verstraeten et al., 2006) and North Rhine Westphalia (Fiener et al., 2013). The estimation of erosivity density moving average contributes to identify regional trends of rainfall intensity and possible signals of climate change.

3.4. Monthly rainfall erosivity and soil erosion risk

The monthly erosivity density identifies periods (when) and hotspots (where) of intense rainstorms compared to low intensity rainfalls. The temporal distribution of rainfall erosivity can be very important for identifying the high risky periods when soil exposure coincides with high erosive months (Sheridan and Rosewell, 2003). Almost 60% of the annual rainfall erosivity in Greece is accounted in 4 months period (October–January). The monthly distribution of rainfall erosivity in combination with seasonal land cover and management changes (C-factor) contributes to monthly soil erosion prediction by using RUSLE based models such as the G2 soil erosion model. Moreover, the development of seasonal erosivity maps contributes to the estimation of seasonal soil loss ratios (Panagos et al., 2015c). The identification of hotpots for a specific time of the year will be a useful tool for policy makers to guide investments for soil protection against erosion and prioritise actions for effective remediation. For example, tillage should be avoided in the most erosive period (November) in areas with high R-factor. On the contrary, the clean tilled row crops (corn, sugar beets, cotton, and sunflowers) are not susceptible to erosion in Thessaly plain during April–May as erosivity is minimum during this period. With the publication of this study, the datasets (monthly R-factor, erosivity density, standard error, etc) are available in the European Soil Data Centre (ESDAC, 2012).

Greece is characterised by a high proportion (26.5%) of bare soil (Eurostat, 2014a). At regional level, Ipeiros has even a proportion of 57% of bare soil in agricultural lands (Eurostat, 2014a). The combination of high erosivity density in Ipeiros and western Greece with bare soil coverage may cause severe soil loss and have detrimental impacts on the resource soil. The habit of farmers in Greece to burn the crop residues during summer (Barbayiannis et al., 2011) followed by high erosivity density in autumn may be judged negative with respect to soil conservation. A positive land use statistic is that the proportion of permanent grasslands is by 50% higher in the regions with the highest rainfall erosivity density (Western Greece, Peloponnesus and Western Crete) compared to the average percentage of grasslands cover. However, a negative aspect of grassland management in Greece is that around 71% of the grasslands are grazed for a period longer than 10 months, which is one of the highest in European Union both in terms of duration and proportion.

Tillage practice is another soil erosion risk factor with high spatio-temporal variability. It may be incorporated in the RUSLE model via the P-factor, which accounts for soil conservation practices or proposed as a new management factor (as part of C-factor). According to the tillage practices agro-environmental indicator (Eurostat, 2014b), only 2% of agricultural land in Greece is under zero tillage and conservation tillage is applied for around 20% of the area. Both values are lower than the European Union averages. However, the conventional tillage has quite low shares in high erosive regions such as Peloponnesus (44%), Crete (55%) and Western Greece (66%).

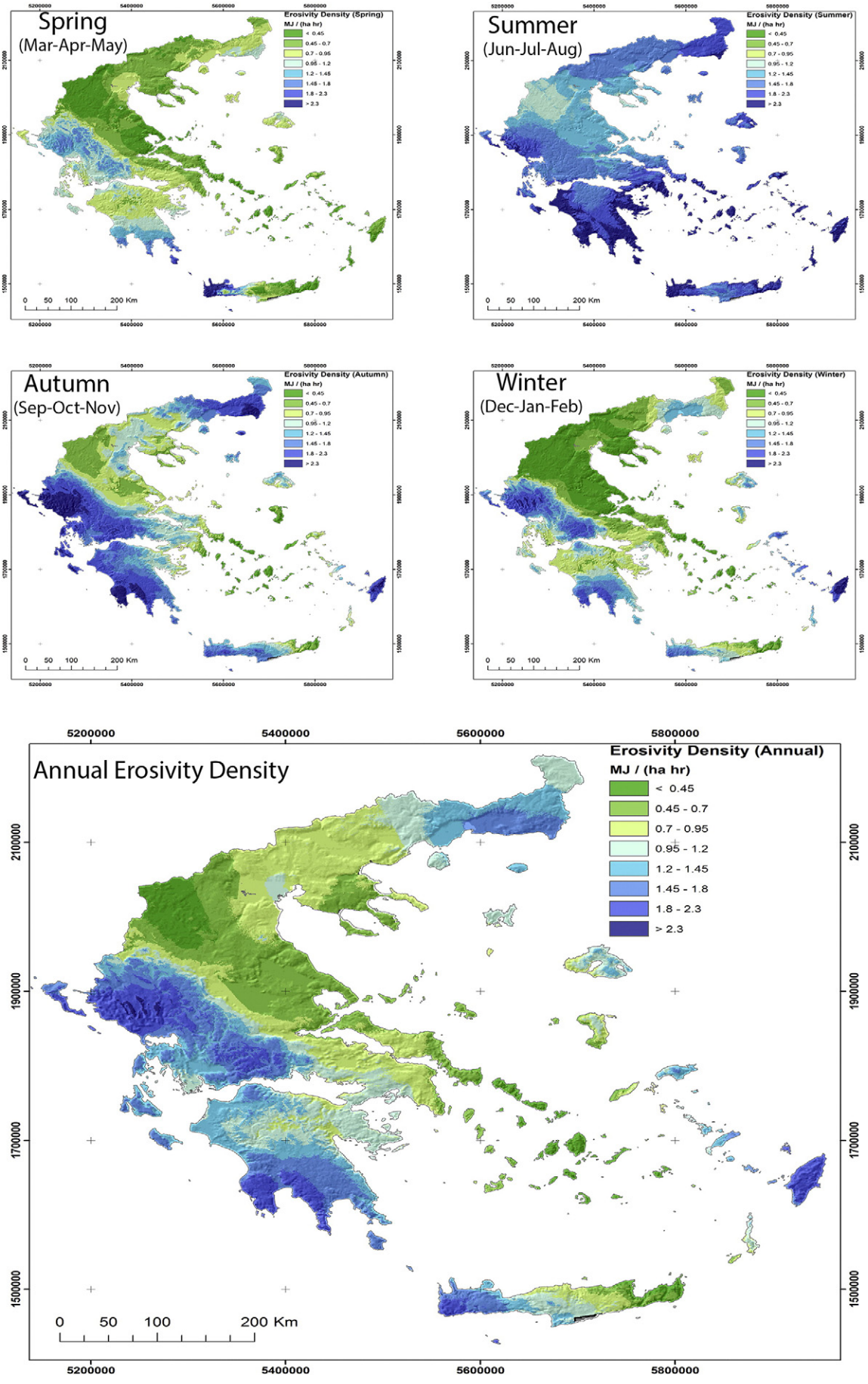

Fig. 6. Seasonal erosivity density (rainfall erosivity per mm of precipitation).

4. Conclusions

The monthly rainfall erosivity maps (based on high temporal resolution data) and the following seasonal erosivity density assessment for a whole country (Greece) are the greater advancements in this study. Besides mapping, rainfall erosivity and erosivity density are important for soil erosion risk assessment, application of soil conservation measures and regional climate change trends.

Monthly rainfall erosivity in Greece has a high intra-annual variability with the highest value in November of 144.6 MJ mm ha^{-1} h^{-1} $month^{-1}$ and lowest in July with 37.1 MJ mm ha^{-1} h^{-1} $month^{-1}$. In Greece, the wet period especially October, November and December are the most erosive months. The wet period (October–March) contribution to the total annual rainfall erosivity is around 73%.

The spatial interpolation model performed well during the high erosive months while it had relatively 'poor' performance during summer months due to few and unpredictable rainstorms events. The erosivity density analysis and the monthly R-factor regression functions based on station data indicates that rainfall erosivity per precipitation amount is higher (more rainstorms) during the period June–December. The monthly R-factor regression functions are recommended only for other areas in Greece where detailed precipitation records are scarce.

The average annual R-factor in Greece is 807 MJ mm ha^{-1} h^{-1} $year^{-1}$. The spatial variability of rainfall erosivity is high in Greece with the Western part and Peloponnesus having the highest values while the eastern coast, Macedonia region, Thessaly and Cyclades have relatively low R-factor. The East–West gradient of rainfall erosivity has different patterns per month with smoother distribution during summer and high variability during winter months. The seasonal erosivity density improves the usefulness and effectiveness of R-factor by identifying the areas (Western Greece, South-west Peloponnesus, west Crete, and Dodecanese) and seasons (autumn) of the most intense and erosive rainfalls. Moreover, the spatio-temporal analysis of erosivity density demonstrates that it is impossible to spatially predict the R-factor per month exclusively based on precipitation levels.

To conclude, the spatio-temporal maps of R-factor are useful (considering the proposed uncertainties) for agronomists to identify the locations and periods when highest erosivity risk meets susceptible crops and may allow for timely soil conservation measures such as zero tillage and crop residues. Finally, this study in Greece showed the potential to compute the monthly rainfall erosivity in European Union by using the recently published Rainfall Erosivity Database on the European Scale (REDES).

Conflict of interest

The authors confirm and sign that there is no conflict of interests with networks, organisations, and data centres referred in the paper.

Acknowledgements

The authors would like to thank Irene Biavetti for the revision of the article from a linguistic point of view and for her support in graphical interface. The authors would also like to acknowledge the "Hydroscope" service for providing access to their data.

Appendix A. Supplementary data

Supplementary data to this article can be found online at http://dx.doi.org/10.1016/j.catena.2015.09.015.

References

Ballabio, C., Panagos, P., Montanarella, L., 2014. Spatial Prediction of Soil Properties at European Scale Using the LUCAS Database as a Harmonization Layer. GlobalSoilMap: Basis of the Global Spatial Soil Information System - Proceedings of the 1st GlobalSoilMap Conference, pp. 35–40.

Barbayiannis, N., Panayotopoulos, K., Psaltopoulos, D., Skuras, D., 2011. The influence of policy on soil conservation: a case study from Greece. Land Degrad. Dev. 22 (1), 47–57.

Bartzokas, A., Lolis, C.J., Metaxas, D.A., 2003. A study on the intra-annual variation and the spatial distribution of precipitation amount and duration over Greece on a 10-day basis. Int. J. Climatol. 23, 207–222.

Bonilla, C.A., Vidal, K.L., 2011. Rainfall erosivity in Central Chile. J. Hydrol. 410 (1–2), 126–133.

Brown, L.C., Foster, G.R., 1987. Storm erosivity using idealized intensity distributions. Trans. ASAE 30, 379–386.

Colombo, S., et al., 2005. Designing policy for reducing the off-farm effects of soil erosion using choice experiments. J. Agric. Econ. 56 (1), 81–96 ((16), 1 January).

Dabney, S.M., Yoder, D.C., Vieira, D.A.N., Bingner, R.L., 2011. Enhancing RUSLE to include runoff-driven phenomena. Hydrol. Process. 25 (9), 1373–1390.

Diodato, N., Verstraeten, G., Bellocchi, G., 2014. Decadal modelling of rainfall erosivity in Belgium. Land Degrad. Dev. 25 (6), 511–519.

ESDAC, 2012. European soil data centre Accessed at: http://esdac.jrc.ec.europa.eu.

Eurostat, 2014a. Soil cover agro-environmental indicator Accessed at: http://ec.europa.eu/eurostat/statistics-explained/index.php/Agri-environmental_indicator_-_soil_cover.

Eurostat, 2014b. Tillage practices agro-environmental indicator Accessed at: http://ec.europa.eu/eurostat/statistics-explained/index.php/Agri-environmental_indicator_-_tillage_practices.

Fiener, P., Neuhaus, P., Botschek, J., 2013. Long-term trends in rainfall erosivity-analysis of high resolution precipitation time series (1937–2007) from Western Germany. Agric. For. Meteorol. 171-172, 115–123.

Foster, G.R., Yoder, D.C., Weesies, G.A., McCool, D.K., McGregor, K.C., Bingner, R.L., 2008. Draft User's Guide, Revised Universal Soil Loss Equation Version 2 (RUSLE-2). USDA-Agricultural Research Service, Washington, DC (Accessed at http://fargo.nserl.purdue.edu/rusle2_dataweb/userguide/RUSLE2_User_Ref_Guide_2008.pdf).

Goovaerts, P., 1999. Using elevation to aid the geostatistical mapping of rainfall erosivity. Catena 34, 227–242.

Hastie, T., Tibshirani, R., 1986. Generalized additive models. Stat. Sci. 1, 297–318.

Hatzianastassiou, N., Katsoulis, B., Pnevmatikos, J., Antakis, V., 2008. Spatial and temporal variation of precipitation in Greece and surrounding regions based on global precipitation climatology project data. J. Clim. 21 (6), 1349–1370.

Hijmans, R.J., Cameron, S.E., Parra, J.L., Jones, P.G., Jarvis, A., 2005. Very high resolu-tion interpolated climate surfaces for global land areas. Int. J. Climatol. 25, 1965–1978.

HNMS, 2014. Hellenic National Meteorological Service Web address available at: http://www.hnms.gr.

Kambezidis, H.D., Larissi, I.K., Nastos, P.T., Paliatsos, A.G., 2010. Spatial variability and trends of the rain intensity over Greece. Adv. Geosci. 26, 65–69.

Kinnell, P.I.A., 2010. Event soil loss, runoff and the universal soil loss equation family of models: a review. J. Hydrol. 385, 384–397.

Köoppen, W.P., 1918. Klassification der klimate nach temperatur, nieduschlag und Jahreslanf. Petermanns Geogr. Mitt. 64 (193–203), 243–248.

Meusburger, K., Steel, A., Panagos, P., Montanarella, L., Alewell, C., 2012. Spatial and temporal variability of rainfall erosivity factor for Switzerland. Hydrol. Earth Syst. Sci. 16 (1), 167–177.

Nastos, P.T., Matsangouras, I.T., Chronis, T.G., 2014. Spatio-temporal analysis of lightning activity over Greece — preliminary results derived from the recent state precision lightning network. Atmos. Res. 144, 207–217.

Nyssen, J., et al., 2005. Rainfall erosivity and variability in the Northern Ethiopian Highlands. J. Hydrol. 311 (2005), 172–187.

Oliveira, P.T.S., Wendland, E., Nearing, M.A., 2013. Rainfall erosivity in Brazil: a review. Catena 100, 139–147.

Panagos, P., Ballabio, C., Borrelli, P., Meusburger, K., Klik, A., Rousseva, S., Tadić, M.P., Michaelides, S., Hrabalíková, M., Olsen, P., Aalto, J., Lakatos, M., Rymszewicz, A., Dumitrescu, A., Beguería, S., Alewell, C., 2015b. Rainfall erosivity in Europe. Sci. Total Environ. 511, 801–814.

Panagos, P., Borrelli, P., Poesen, J., Ballabio, C., Lugato, E., Meusburger, K., Montanarella, L., Alewell, C., 2015a. The new assessment of soil loss by water erosion in Europe. Environ. Sci. Pol. 54, 438–447.

Panagos, P., Karydas, C.G., Ballabio, C., Gitas, I.Z., 2014. Seasonal monitoring of soil erosion at regional scale: an application of the G2 model in Crete focusing on agricultural land uses. Int. J. Appl. Earth Obs. Geoinf. 27B, 147–155.

Panagos, P., Karydas, C.G., Gitas, I.Z., Montanarella, L., 2012. Monthly soil erosion monitoring based on remotely sensed biophysical parameters: a case study in Strymonas river basin towards a functional pan-European service. Int. J. Digit. Earth 5 (6), 461–487.

Panagos, P., Meusburger, K., Ballabio, C., Borrell, I.P., Begueria, S., Klik, A., Rymszewicz, A., ... Alewell, C., 2015c. Reply to the comment on "Rainfall erosivity in Europe" by Auerswald et al. Sci. Total Environ. 532 (2015), 853–857.

Pimentel, 2006. Soil erosion: a food and environmental threat. Environ. Dev. Sustain. 2006 (8), 119–137.

Pnevmatikos, J.D., Katsoulis, B.D., 2006. The changing rainfall regime in Greece and its impact on climatological means. Meteorol. Appl. 13, 331–345.

Renard, K.G., et al., 1997. Predicting Soil Erosion by Water: A Guide to Conservation Planning With the Revised Universal Soil Loss Equation (RUSLE) (Agricultural Handbook 703). US Department of Agriculture, Washington, DC, p. 404.

Renschler, C.S., Mannaerts, C., Diekkruger, B., 1999. Evaluating spatial and temporal variability in soil erosion risk — rainfall erosivity and soil loss ratios in Andalusia, Spain. Catena 34 (3–4), 209–225.

Sakellariou, A., Koutsoyiannis, D., Tolikas, D., 1994. HYDROSCOPE: Experience from a Distributed Database System for Hydrometeorological Data. International Conference on Hydraulic Engineering Software, Hydrosoft, Proceedings, 2, pp. 309–316.
Sheridan, G.J., Rosewell, C.J., 2003. An improved Victorian erosivity map. Aust. J. Soil Res. 41 (1), 141–149.
Tolika, K., Maheras, P., 2005. Spatial and temporal characteristics of wet spells in Greece. Theor. Appl. Climatol. 81, 71–85.
Verstraeten, G., Poesen, J., Demaree, G., Salles, C., 2006. Long-term (105 years) variability in rain erosivity as derived from 10-min rainfall depth data for Ukkel (Brussels, Belgium): implications for assessing soil erosion rates. J. Geophys. Res. 111 (D22).
Wischmeier, W., Smith, D., 1978. Predicting Rainfall Erosion Losses: A Guide to Conservation Planning. Agricultural Handbook No. 537. U.S. Department of Agriculture, Washington DC, USA.
Wood, S.N., 2006. Generalized Additive Models: An Introduction with R. Chapman & Hall/CRC, Boca Raton, USA.